Integrating Data Across Oscillatory Power Bands Predicts the Epileptogenic Zone: the Frequency Range Explorer Epileptogenic Zone (FREEZ) Identification Algorithm

Authors: Sean O'Leary[1,†], Anne-Cecile Lesage[1,†], Liliana Camarillo-Rodriguez[1], Oliver Zhou[1], Diosely Silveira[2], Jiefei Wang[3], Sameer A. Sheth[4], Michael S. Beauchamp[5], Zhengjia Wang[5], John F. Magnotti[5], Patrick J. Karas[1,6]

Abstract

Epilepsy affects over 70 million people globally. One-third of people with focal epilepsy have drug-resistant epilepsy. Identification and removal of the site of onset of seizures, termed the epileptogenic zone (EZ), is the most successful treatment to stop seizures in these people. Implanting electrodes into the brain with intracranial electroencephalography (iEEG) is the gold standard diagnostic test for identifying the EZ. But identification of the EZ with iEEG remains challenging in many cases. We developed a novel computational methodology that integrates mean power across delta, theta, alpha, beta, gamma, and high gamma frequencies over time to identify the EZ. A machine learning model was trained to predict electrodes within the EZ using publicly available data from 21 patients. In patients that were seizure free after surgery, electrodes within the EZ had significantly higher area under the curve (AUC) for mean power over time in the first 20 seconds after a seizure compared to electrodes outside the EZ in the alpha ($p = 0.001$), beta ($p = 0.001$), gamma ($p < 0.0001$), and high gamma ($p = 0.0003$) ranges. Additionally, electrodes within the EZ in patients that became seizure-free after surgery had significantly higher AUC compared to electrodes marked within the EZ in patients who did not become seizure-free after surgery in the gamma ($p = 0.0006$) and high gamma ($p < 0.0001$) power ranges. Leave-one-out patient cross validation of the machine learning model yielded a 95.7% positive predictive value and 80.6% specificity for identifying electrodes within the epileptogenic zone, and 90.5% accuracy for predicting seizure outcome based on a planned resection.

We implemented this algorithm into the open-source software tool "Reproducible Analysis and Visualization of iEEG" (RAVE) to enable users to reproduce our results and implement this methodology with new datasets, creating a software module we title FREEZ. The software facilitates quantification of the spectral power changes during seizures, including displaying time-frequency spectrograms and projecting results across patient-specific 3D brain maps. Users can also adjust parameters for visualizing multiple frequency ranges from various time regions around seizure onsets in a web-browser-based interface.

Affiliations:
[1]Department of Neurosurgery, University of Texas Medical Branch, Galveston, TX, USA
[2]Department of Neurology, University of Texas Medical Branch, Galveston, TX, USA

[3]Department of Biostatistics & Data Science, University of Texas Medical Branch, Galveston, TX, USA
[4]Department of Neurosurgery, Baylor College of Medicine, Houston, TX, USA
[5]Department of Neurosurgery, University of Pennsylvania, Philadelphia, PA, USA
[6]Department of Neurosurgery, University of Texas MD Anderson Cancer Center, Houston, TX, USA

[†]These authors contributed equally to this work

Corresponding Author's name and current institution:

Patrick Karas
301 University Blvd, JSA 9.300
Galveston, TX 77555-0517
pjkaras@utmb.edu

Running Title: Frequency Range Explorer Epileptogenic Zone (FREEZ) Identification Algorithm

Key Words: drug-resistant epilepsy, epileptogenic zone localization, iEEG power analysis, multi-taper, FREEZ, RAVE

Introduction

Drug resistant epilepsy (DRE) is estimated to affect approximately 33% of patients, defined as failure to achieve sustained seizure freedom following the use of two tolerated and appropriately chosen anti-epileptic drug (AED) regiments.[1,2] DRE is associated with increased mortality rate, with 40% experiencing sudden unexpected death during epilepsy.[3] Surgical treatments offer the potential of seizure freedom for DRE patients, with reported seizure freedom rates of 58% to 78% following resection of the epileptogenic zone (EZ).[4] Historically, the EZ has been characterized as the portion of the brain that is both required and adequate for attaining freedom from seizures after surgical removal.[5,6] In cases when non-invasive exams (electroencephalography EEG,) are not conclusive the clinical standard-of-care for EZ localization is visual interpretation of seizures from implanted intracranial electroencephalography (iEEG) electrode recordings by an epileptologist[7]. Epileptiform discharges are visually identified from iEEG recordings and correlated with their anatomic location and the patient's clinical features to identify the EZ. Seizure outcomes (seizure freedom versus continuation of seizures) after surgery are suggestive of whether the EZ was correctly identified and removed during surgery or not. Using surgical outcomes as validation, computational epileptogenic zone identification algorithms (CEZIAs) have been developed to help clinicians identify the EZ. Different CEZIAs analyze different subsets of features selected from iEEG recordings, including the timing and anatomic distribution of these signals, extracting a subset of "anatomical-electro-clinical correlations" that are central to defining the EZ. CEZIAs range from basic signal processing on individual channels (univariate) to examining channel pairs (bivariate) and whole-network connectivity (multivariate)[8].

Several univariate methods are based on the analysis of the spectral content of the IEEG signals at seizure onset. They rely on the different frequency patterns that have been clinically

observed[9,10]. Some CEZIAs demonstrated the correlation between EZ localization and high power in the beta frequency range[11,12]. Bartolomei *et al.*[13]developed the epileptogenic index method which relies on assessing the timing of changes in the ratio of energy between fast (beta and gamma range) and slow activities (alpha and theta range). In Grinenko *et al.*[14], correlation between the association of multi-band fast activity and low frequency suppression with EZ localization was reported. In Izumi *et al.*[15], the relationship between cooccurrence of ictal direct current shifts (icDCs) and ictal high frequency oscillations and EZ localization was investigated. These studies demonstrate a complex interplay of neural activity across different frequency bands during seizure onset. However, a unified method to consider all frequency patterns correlating with EZ localization is missing.

Among spectrogram analysis methods, multitaper spectrogram analysis (MSA) provides accurate frequency resolution[16]. However, despite the existence of publicly available libraries for Spectrogram Analysis (SA) including the multitaper_toolbox[17], there is no integration with iEEG localization and signal processing tools. Also, there is no integration that is paired with visualization functionalities to explore and analyze the correlation of EZ localization and increased relative mean power: spatiotemporal visualization of the mean relative power by electrodes and brain mapping of multitaper spectrogram analysis (MSA) results.

To design a tool for aiding the EZ localization process through a unified MSA, we developed FREEZ (the Frequency Range Explorer Epileptogenic Zone) a web-based visualization tool to quantify and predict electrode classification and seizure outcomes based on changes in the spectral power around the seizure onset zone. FREEZ also allows for multi-patient analysis through script-based pipelining to generate both results as well as provide statistical analysis and prediction using ensemble machine learning[18] stacking models built on several frequency range analysis. The advantage of FREEZ is that it is opensource, does not rely on expensive commercial licenses and is integrated into RAVE **R**eproducible **A**nalysis and **V**isualization of intracranial **E**EG[19], an NIH platform. In this paper, we validate the performance of our tool to assist EZ localization by analyzing mean relative power on the publicly available Fragility multi center dataset[11].

Material and Methods

Patient Data and Selection

The Fragility multi center dataset[11], available publicly on the OpenNeuro platform, encompasses data from 35 patients distributed across four centers (NIH, JHH, UMCC and UMF). The iEEG data is structured in the BIDS format. Electrode names and classification by epileptologists in the seizure onset zone are available. However, electrode localization is not available. The iEEG signal data is in the BrainVision format. A file features event markers annotated by clinicians that indicate the timing of clinical events and the onset/offset for each seizure, both clinically and electrographically. These seizures are marked according to standard procedures within the clinical epilepsy workflow. In in this paper study, patients met the following criteria: (1) they underwent resection or laser ablation surgery guided by intracranial EEG using subdural grids, strips, and depth electrodes (ECoG); (2) they had at least one seizure recorded during intracranial monitoring,

allowing for confirmatory testing of selected channels; (3) their recordings were at frequencies of 500 Hz or higher, suitable for high-range frequency analysis; and (4) detailed surgical outcomes, including Engel scores, were available. After exclusions, 21 patients remained in the study for a quantitative analysis focused on the relationship between MSA and the EZ. A total of 21 patients were included. The mean age at epilepsy onset was 19.5 ± 12 years (range: 13-59), and the mean age at the time of surgery was 36.39 ± 12.13 years (range: 13-59). The mean epilepsy duration before surgery was 16.89 years (range: 4-41). The cohort included 9 males, 9 females, and 3 patients with unspecified sex. All patients underwent ECoG, with an average of 3.05 ± 0.84 ictal events recorded per patient (range: 1-4). Surgical targets were predominantly in the temporal lobe (N = 17), followed by the frontal lobe (N = 2) and the parietal lobe (N = 2). Post-surgery, 14 patients achieved seizure freedom (Engel I), while 7 did not. Among the non-seizure-free patients, 3 were classified as Engel II, 1 as Engel III, and 3 as Engel IV [see ***Supplementary Table 1***]. As in the study by Li *et al.*[11], we assume for the validation of our EZ localization tools that the annotated SOZ electrodes are inside the resected area for all patients and that they are a good estimate of the EZ in case of seizure freedom outcome.

iEEG data preprocessing in RAVE and YAEL

Raw signal has been preprocessed in RAVE 2[19]. Data was notch filtered and common average referenced. These steps can be either be applied using the RAVE 2 GUI (graphical user interphase) or automatized with RAVE 2 pipelines which allow for script-based analysis without GUI use. Electrode localization can be either preprocessed with YAEL[20] (patient specific) or from standardized prelocalized format (MNI) on a template 3D brain.

Multitaper spectral analysis

To carry out MSA, we implemented the computation of spatiotemporal heatmap of electrode mean power for user-defined frequency range in R. The MSA is based on the multitaper R library[17] which provide tools to compute the multitaper Fourier transform[21] in an efficient parallel implementation. To generate MSA results, the basic parameters include the step size or window length for analysis with respective default values 2.5s and 0.5s. The main lobe's bandwidth, in turn, defines the frequency resolution or the smallest detectable frequency difference, and its default value is set to 3 for optimal resolution. Additionally, the time-half bandwidth product is determined by multiplying the window's length (N seconds) by half of the main lobe's bandwidth (BW/2). These values ensure accuracy for a wide range of frequencies[11,17]. Advanced customization choices include setting the number of DPSS tapers used for spectrogram computation, specifying the minimum allowable NFFT size for manual zero-padding adjustment to optimize the Fast Fourier Transform (FFT) computation, selecting taper weights (options include "unity," "eigen" for taper contribution weighted by eigenvalues, or "adaptive" to minimize broadband leakage), choosing a detrend method ("linear" for fitting a linear model and subtraction, "constant" for zero-mean data, or "off" for no detrending), and configuring the number of parallel CPU cores for processing.

Statistical analysis of correlation between spectral features and EZ localization

We have implemented multi-patient pipelining in RAVE[19] to allow for generation of MSA mean power heatmap results in .csv format for statistical analysis of correlation with EZ classifications. We tested this pipelining on the Fragility public data set, generating heatmaps 0s from seizure onset to 20s after seizure onset, with mean subtract baselining for all analyzed seizure to a time window -30s to -20s before seizure onset. We computed multitaper heatmap across six frequency bands (delta, theta, alpha, beta, gamma, and high gamma).

The resultant heatmaps were further statistically analyzed for each patient through both an average power over time plot as well as a statistic over time plot of the 10th through 100th power percentiles (in steps of 10) for two groups of electrodes: EZ and non-EZ-labeled electrodes.

The mean and standard deviation were calculated for the area under the curve (AUC) of the average power over time plot for EZ and non-EZ labeled electrodes stratified by post-surgical seizure freedom outcome. To evaluate significant differences in metrics between electrodes classified as within or outside the epileptogenic zone (EZ) for both seizure-free and non-seizure-free patients, pairwise Wilcoxon Rank Sum tests were conducted. Additionally, we compared metrics between seizure-free and non-seizure-free conditions across EZ and non-EZ channel average power AUCs. A Bonferroni correction was applied to all p-values to adjust for multiple testing, enhancing the reliability of the statistical assessments for multiple pairwise testing.

Ensemble machine learning method to combine multi-band frequency analysis for electrode classification and patient outcome prediction

We employed a trained stacked random forest ensemble (SRFE) machine learning approach to predict the epileptogenic zone (EZ) on a selected patient seizure condition. Specifically, it necessitates a 20-second temporal window post-seizure onset for analysis, incorporating a series of random forest algorithms, which have been trained on the seizure-free cohort from the Fragility[11] dataset. The algorithm processes individual predictions across six distinct frequency bands: delta (0.5-4 Hz), theta (4-8 Hz), alpha (8-13 Hz), beta (13-30 Hz), gamma (30-90 Hz), and high gamma (90–256 Hz), and subsequently aggregates these predictions to inform a final SRFE model that synthesizes the comprehensive spectral data to produce the final EZ predictions. We tested this model with first a large random forest model set to generate 100 decision trees for time-frequency features, with an additional feature weighting each frequency band by summing the power of all time windows per band. This was compared with the results from training 6 independent random forest models with 100 decision trees on each frequency band and averaging the outcome, as well as against an SRFE model using the H2O R package to make final predictions from the output probabilities. Thresholds for the prediction were analyzed, and the most specific model was selected for final analysis. The final model was then used to calculate the algorithm's

performance metrics: AUC, accuracy, specificity, sensitivity, positive predictive value (PPV), and negative predictive value (NPV). For all cross validation, leave-one-out patient cross validation was employed, with majority voting (≥ 50%) across different seizure conditions for each patient to select final predictions. In our analysis, the importance of each feature was determined by extracting the feature coefficient from the SRFE model. A larger coefficient for base models indicates a more significant impact on the SRFE model in enhancing prediction accuracy, thereby helping to prioritize which of the six frequency band features are most influential in predicting EZ classification. We then trained the final SRFE model on all seizure free patients, and subsequently tested on non-seizure free patients to confirm selection of EZ electrodes corresponded to the ground truth of seizure freedom when removed.

Patient outcomes were predicted using time-series plot analysis. In this process, power percentiles of the EZ channels, ranging from the 10th to the 100th percentile in 10-percent increments, were normalized on a 0 to 1 scale. These normalized values were then divided by their corresponding percentiles from the non-EZ channels, also scaled between 1 and 10, resulting in a set of ratios. These ratios, representing relative power differences for each percentile across all plots, were tailored for each patient, condition, and frequency band. Initially, these ratios were used to train a random forest model consisting of 100 decision trees for each frequency band. Subsequently, correlations between the predictions across frequency bands were calculated using the Pearson correlation coefficient. Following this, an SRFE (Stacked Random Forest Ensemble) model was constructed using the H2O R package, incorporating stacked random forests from each of the six frequency ranges. The cutoff threshold for predictions was established based on the maximum model accuracy. For all cross-validation procedures, a leave-one-out patient cross-validation method was used, along with majority voting (≥ 50%) across different seizure conditions for each patient to finalize predictions.

FREEZ module: a toolbox for visualization of correlation analysis between spectral features and EZ localization

The different processes described in the previous subsections have been integrated and are freely available through the FREEZ module GUI (Frequency Range Explorer Epileptogenic Zone) for visualization after processing and reproducibility of this study results: frequency range MSA mean power heatmap, statistical analysis of correlation between spectral features and EZ localization for individual patients through electrode grouping and prediction results of SFRE for electrode localization of an individual patient. FREEZ is integrated as a RAVE module written in R programming language, HTML (hypertext markup language), CSS (cascading style sheets), JavaScript, and shell.[22] RAVE integration allows users to run on laptops, desktops, or in the cloud, with seamless integration between platforms as all module interaction is performed through a web browser.[22] Because all computing in RAVE can be performed on any server or user machine, interaction with the module does not require independent computation.[22] IEEG data set have to be preprocessed in RAVE 2 as described in the second subsection of this section for further processing in FREEZ.

The advanced parameters of an MSA to compute mean power in a user-defined frequency range can be toggled in the FREEZ GUI (***Supplemental Figure 1 A and B)***. Following processing of the multi-taper results, the user can choose the epoch time window around the seizure offset. The user can choose between several conditions of the RAVE preprocessed signal e.g. ictal signal of different recorded seizures, and toggle between conditions for analysis. The user can also mean subtract baseline the heatmaps to a selected baseline condition, with the option the duration from the start of the baseline condition that the user wishes to utilize, where $X = X - \text{mean}(X_B)$, where again X represents the original heatmap and X_B the selected baseline condition for the selected baseline duration. The options for this are presented in ***Supplemental Figure 1C***. Frequency ranges and time axis can be modified for the analysis condition, with the analysis options allowing for sliding bars to be utilized for tailoring the analysis results. We also provide buttons for preset frequency ranges of interest for user convenience encompassing Delta [0.5-4 Hz], Theta [4-8 Hz], Alpha [8-13 Hz], Beta [13-30 Hz], Gamma [30-90 Hz] and High Gamma [90+ Hz] frequency ranges. The user can also define additional analysis frequency ranges.

Plotting options are also given with the ability for the user to choose between a non-normalized heatmap view, or a min-max normalization of the heatmap by time window. For the min-max normalization of the heatmap by time window, a mean power value per time window is computed and max-normalized by time window in the range [-1:1], e.g. the electrode with value one is the one with highest power in the time window: $X_{norm}(i,j) = X(i,j) - \min(X_{Wt}) / \max(X_{Wt}) - \min(X_{Wt})$ where X represents the original heatmap, $X_{i,j}$ is the element at row i and column j of X, W_t represents the time window t, X_{Wt} represents the submatrix of X within time window W_t, $\text{Max}(W_t)$ represents the maximum value within the time window W_t, and X_{norm} represents the final normalized data matrix. Color maps can be selected to change all the plotting value scales.

The user can also input electrodes deemed SOZ or Resect for plotting, with SOZ coded blue, Resect Purple, and contacts with overlap between the input Resect and SOZ colored Green on the y axis. The resultant power-over-time per electrode plot can also be grouped by provided Resect or SOZ contacts to aid in visualization through the grouping of channels of interest, as well as have the electrode labels toggled between numeric labels. The user can also convert the power units (P) supplied by the multitaper result into decibels (dB), where $\text{dB}=10 \times \log_{10}(P)$. These options are all provided in ***Supplemental Figure 1E***. The power over time plot as seen in ***Figure 1D*** can be correlated with the raw signal result in ***Figure 1C*** for visualization of the spectral features extracted from signal data by the multitaper. Electrodes can be selected by their number and be colored by labels, here in blue for the electrodes annotated as SOZ by epileptologists. Users can see either their number from the channel files in the BIDS format or their name as in Figure 1C. Heatmap visualization can be toggled to display electrodes grouped as resected on top and the remaining electrodes on the bottom. This can be useful to check visually that marked electrodes correlate with high relative power.

The module GUI provides also visualization of the statistical analysis of the MSA heatmap results by electrodes grouping (see Figure 1E and 1F). The power over time plot as seen in ***Figure 1D*** can be correlated with the raw signal result in ***Figure 1C*** for visualization of the spectral features extracted from signal data by the multitaper. FREEZ GUI offer the visualization of the average power over time plot for PT01 with specified EZ channels. The statistic over time plot can also be stratified, with stacked heatmaps for other, resect, and/or soz channels divided by a red line.

Moreover, the user can visualize the quantile statistics over time plot which provides additional analysis of differences in the power between selected electrodes [***Figure 1F***].

FREEZ offers a similar brain visualization tool than YAEL[18]. It uses open-source R code to process the workflow and the shiny package for the user interface. FREEZ provides the ability to visualize electrodes on a template, or patient specific brain model. Additionally, we provide an electrode projection functionality to take in account brain shape variability (see ***Figure 1A and 1B***). FREEZ allows patient specific visualization of brain cortex surface mesh in the FreeSurfer format[23]. This data can be computed using the FreeSurfer software and patient specific T1 MRI (magnetic resonance imaging) imaging. With FREEZ brain mapping functionality, the MSA heatmap can be projected over the patient specific or template 3D brain for visualization of anatomical position, as well as location of selected resect and soz channels, and temporal analysis through a sliding bar of changes in heatmap values over time allowing for viewing of the dynamic evolution of the heatmap, color coded based on the color template selected by the user [***Figure 1B***].

Finally, FREEZ allows to pipeline the whole workflow for (see ***Figure 2***) through integration to the RAVE 2 framework for multi-patient analysis.

Data Availability

The source repository is accessible on https://github.com/seanmnoleary/rave-pipelines/tree/sean_update/modules/multitaper_explorer with installation guidelines for the Windows, MacOS and Linux platforms on https://openwetware.org/wiki/Karas_Lab. The web page https://openwetware.org/wiki/RAVE provides documentation to use the software and integrate it for signal preprocessing and electrode localization with two open-source software: RAVE 222 and YAEL24. Users can reach out for help about installation and software use in a dedicated Slack support channel

Results

FREEZ allows multi-component visual and statistic assessment of correlation between MSA results and EZ localization for individual patients

Figure 1 demonstrates how the visualization functionalities of FREEZ can be used for a multi component analysis of the correlation between MSA results and EZ localization for an individual patient, here patient PT01. Figure 1C and 1D demonstrate how the MSA heatmap results correlates with spectral patterns in the raw signal. Here solely the electrodes marked in blue as in the EZ display high power in the gamma frequency range, thus the heatmap can be used to predict visually this patient seizure outcome as a true positive. Figures 1E and 1F allow another confirmation of this true positive prediction thanks to statistical analysis of two groups EZ and non-EZ labelled electrodes.

For six patients out of the twenty-one patients used in this study, we were able to retrieve patient-specific MRI imaging, patient specific cortex and electrode localization from the patient data set used in Diamond *et al.*[25] (PT01, PT2, PT3, PT6, PT14, PT15). 3D brain mapping in FREEZ for patient PT01 confirms the correlation between high power in the gamma range and EZ localization (see Figure 1A and 1B).

MSA multi-patient analysis using FREEZ pipelines reveals that high power in alpha, beta, gamma and high gamma range correlates with EZ localization

We used the pipelining functionalities of FREEZ on the Fragility Data Set[11] to generate heatmaps in six frequency ranges for 21 patients with a total of x seizure conditions. Electrodes labeled as resected EZ had a significantly higher area under the curve (AUC) for mean power over time in the first 20 seconds following seizure onset compared to non-EZ electrodes in seizure-free patients. This was observed in the alpha ($p = 0.001$), beta ($p = 0.001$), gamma ($p < 0.0001$), and high gamma ($p = 0.0003$) frequency ranges. Additionally, EZ electrodes in seizure-free patients had a significantly higher AUC than EZ electrodes in non-seizure-free patients for average power over time in the gamma ($p = 0.0006$) and high gamma ($p < 0.001$) frequency ranges [***Figure 3***]. These results highlight that significant spectral information for EZ localization is contained in several frequency ranges MSA. Thus, it justifies combining them through a SFRE model to design an electrode classification tool.

SFRE model performs significantly better than RF models based on individual frequency ranges for electrode classification and patient outcome prediction

We used the multi-patient multi-frequency data generated previously for multipatient statistical analysis to run computational experiments on Random Forest model performance. The optimal threshold for random forest output probabilities was 90.67% [***Figure 4B***]. The prediction of electrodes within the EZ by the SRFE model resulted in 22 true positive predictions within the EZ and one false positive [***Figure 4A***]. True positives were identified in 8 out of the 14 seizure-free patients: PT01, PT02, PT08, PT13, PT15, PT17, UMMC002, and JH105. Feature importance, measured by min-max scaled mean squared error decrease, was highest in the beta range (0.66 ± 0.07), followed by high gamma (0.57 ± 0.08), delta (0.51 ± 0.06), alpha (0.43 ± 0.07), gamma (0.39 ± 0.05), and theta (0.18 ± 0.07). The SRFE model, trained on seizure-free patients and tested on non-seizure-free patients, identified 2 EZ electrodes that were not removed and 3 EZ electrodes that were removed [***Figure 4D***]. The SFRE performs significantly better on electrode classification than an RF model based on individual frequency ranges (see supplementary Figure 2).

After computing an SFRE model based on multi-patient and multi-frequency range analysis, one can visualize electrode classification results on individual patients. Figure 5 illustrate visualization of SFRE model results for four prediction patient cases. It shows the heatmap results in the gamma range for a [0:20] time epoch around seizure onset. The heatmap displays the electrode numbers and the time in seconds, respectively on the y and x axes. Electrodes marked as EZ are highlighted in blue and stacked on the heatmap bottom. Cross marks highlight electrodes that have been classified as EZ by the SFRE model from the multi-patient analysis. We can see on ***Figure 5B*** another visualization of electrode classification result on PT15, a seizure free patient, with high gamma power outside of the resected EZ. As such, our SRFE model selected electrodes both within and outside of resected tissue, resulting in the one false positive result. PT10 demonstrates the predictive power of the SRFE model on a non-seizure free patient, with the expected EZ determined by the SRFE model to be outside of the tissue that was resected. This can be seen by the EZ electrodes on the heatmap bottom that do not correlate well with high relative power in the area predicted by the SRFE model in ***Figure 5C.*** Finally, PT06 represents a patient where potentially sparse sampling resulted in relative spectral power not being predictive of which electrodes should be removed. High relative power is within the removed electrodes, and this correlates the SRFE model predictions as seen in ***Figure 5D***, however the patient was non-seizure free postoperatively.

Finally, patient outcomes were predicted using random forests, each constrained to one of six frequency ranges: delta, theta, alpha, beta, gamma, and high gamma. The highest Area Under the Curve (AUC) was observed for the delta band at 0.77, followed by beta at 0.74, gamma at 0.67, high gamma at 0.57, theta at 0.52, and alpha at 0.51 [***Figure 6A***]. Analysis of the Pearson correlation coefficients between frequency band predictions revealed the strongest correlation between high gamma and gamma ($R^2 = 0.83$), and between beta and alpha ($R^2 = 0.39$). On the other hand, negative correlation was seen between alpha and high gamma ($R^2 = -0.26$) and alpha and gamma ($R^2 = -0.13$) [***Figure 6C***]. Leave-one-out cross validation, using a threshold of 71.22% likelihood from the probability output of the SRFE model, yielded 13 true positives, 6 true negatives, 1 false positive, and 1 false negative [***Figure 6B***]. Overall, the SRFE model achieved an accuracy of 90.48%, with a PPV of 92.86%, NPV of 85.71%, sensitivity of 92.86%, and specificity of 85.71%. Statistics over time plots used for model training when predicting seizure outcome can be seen in ***Figure 6D***, demonstrating both a seizure free patient (PT08) and non-seizure free patient (PT10), both with correctly predicted outcomes by the SRFE model.

Discussion

Our MSA statistical findings on this multi-patient study indicate that specific frequency ranges, particularly suppression in the lower frequencies including delta and theta, and high power in gamma and high gamma, play critical roles in identifying the EZ. These results agree with previous studies computing metrics of this spectral pattern as the Epileptogenic index[13] and the Fingerprint method[14]. The distribution of frequency band feature importance for the SFRE model indicates that the beta, delta and high gamma frequency range are significant predictor which is confirmed by several studies[11,15,25]. Our study confirms complex interplay between spectral features in the EZ. Thus, it is important to consider all frequency bands features for EZ classification generalization on diverse patient data set.

Our multi-patient results suggests that SFRE using MSA of IEEG signals in six different frequency ranges (delta, alpha, theta, beta, gamma and high gamma) is a relevant tool to provide a unified exploration of the correlation between spectral features and EZ localization to automatically classify electrodes. This SFRE performance results encourage further experiments including results based on other features than spectral features like network analysis, phase locked high gamma and source localization.

The FREEZ software developed for this study provides a user-friendly, web-based tool designed to visualize and detect changes in spectral power associated with the onset of a seizure. The tool is tailored to be accessible to both researchers and clinicians, offering a unified platform for informed decision-making during SOZ localization. Developed as a module in R and seamlessly integrated into RAVE, an NIH-supported platform, this tool displays a time-frequency spectrogram and a template brain with a drop-down menu. The 3D brain map allows users to view both the location of electrodes within the brain and those that exhibit biomarker properties.

This tool encompasses a range of valuable features to enhance the user experience. Firstly, it offers a user-friendly interface for both individual patient and multi-patient analysis. Our web-based tool prioritizes usability, ensuring that users, even without programming backgrounds, can easily navigate and utilize its functionalities. Secondly, the tool is seamlessly integrated into the RAVE platform. Our module streamlines the user experience, eliminating the need to switch between multiple platforms for preprocessing, analysis, and result visualization. Further, users can access and implement other RAVE features. Additionally, recognizing the variability inherent in epilepsy data, we provide users with the flexibility to modify settings and parameters as necessary. This adaptability enhances the tool versatility across diverse epilepsy datasets. Lastly, the module goes beyond calculating and displaying results, but enables real-time dynamic adjustments to parameters, facilitating exploration of data. This feature fosters a more dynamic and personalized analysis experience for users, allowing them to tailor their analysis in real-time.

Furthermore, the open-source nature of our software aims to democratize access to advanced epileptic seizure analysis tools and result reproducibility, potentially bridging the gap in epilepsy surgery referrals and facilitating more informed clinical decisions. Through a user-friendly, web-based interface, our tool not only simplifies the analysis process for researchers and clinicians alike but also provides a flexible and dynamic platform for the exploration of epileptic seizure data, enhancing the potential for personalized

Within the current framework of managing patients with DRE, financial impediments are evident, as access to epilepsy surgery is constrained due to the necessity for referrals to a restricted pool of highly specialized physicians.[26–28] By making our open-source software freely available, we hope to address this challenge by allowing for it to be leveraged as a quantitative tool to assist with surgical decision making.

Limitations of this study

For fragility[29] patients the SOZ contacts are an estimation of the resect contacts and the ground truth EZ. Post-surgical T1 MRI was not available. Because XYZ locations were available for only

six patients in the fragility[29] multicenter patients, the exploration of the 3D brain plot functionality for correlation between EZ and MSA heatmap results. We are currently collecting retrospective iEEG data at our institution with patient specific imaging allowing accurate electrode localization (preoperative T1 MRI, CT post implantation) and accurate mapping of the resected area. This data will allow exploration of 3D brain mapping for EZ localization.

The results of this study are limited to twenty-one patients. We plan in the future to test our module on larger patient number thanks to our retrospective patient study. However, the tool is freely available to researchers to perform similar study on independent data set than the one used in this paper. Thus, we encourage further testing of our tool.

Acknowledgements

PJK received funding from the American Association of Stereotactic and Functional Neurosurgeons. We thank Dr Joshua Diamond and Dr Kareem Zaghloul for sharing patients specific imaging and cortex surface mesh corresponding to six out of the 21 patients used in this paper studies.

Funding

This research was funded by the American Society of Stereotactic and Functional Neurosurgery Research Fellowship.

Competing interests

The authors have no personal or institutional interest with regard to the authorship and/or publication of this manuscript.

References

1. Perucca E, Perucca P, White HS, Wirrell EC. Drug resistance in epilepsy. *The Lancet Neurology*. 2023;22(8):723-734. doi:10.1016/S1474-4422(23)00151-5

2. Kwan P, Arzimanoglou A, Berg AT, et al. Definition of drug resistant epilepsy: Consensus proposal by the ad hoc Task Force of the ILAE Commission on Therapeutic Strategies: Definition of Drug Resistant Epilepsy. *Epilepsia*. 2009;51(6):1069-1077. doi:10.1111/j.1528-1167.2009.02397.x

3. Rheims S, Sperling MR, Ryvlin P. Drug-resistant epilepsy and mortality—Why and when do neuromodulation and epilepsy surgery reduce overall mortality. *Epilepsia*. 2022;63(12):3020-3036. doi:10.1111/epi.17413

4. Lamberink HJ, Otte WM, Blümcke I, et al. Seizure outcome and use of antiepileptic drugs after epilepsy surgery according to histopathological diagnosis: a retrospective multicentre cohort study. *The Lancet Neurology*. 2020;19(9):748-757. doi:10.1016/S1474-4422(20)30220-9

5. Jehi L. The Epileptogenic Zone: Concept and Definition. *Epilepsy Curr*. 2018;18(1):12-16. doi:10.5698/1535-7597.18.1.12

6. MacDonald DB, Simon MV, Nuwer MR. Neurophysiology during epilepsy surgery. In: *Handbook of Clinical Neurology*. Vol 186. Elsevier; 2022:103-121. Accessed June 5, 2023. https://linkinghub.elsevier.com/retrieve/pii/B978012819826100017X

7. Gnatkovsky V, De Curtis M, Pastori C, et al. Biomarkers of epileptogenic zone defined by quantified stereo-EEG analysis. *Epilepsia*. 2014;55(2):296-305. doi:10.1111/epi.12507

8. Bernabei JM, Li A, Revell AY, et al. Quantitative approaches to guide epilepsy surgery from intracranial EEG. *Brain*. 2023;146(6):2248-2258. doi:10.1093/brain/awad007

9. Perucca P, Dubeau F, Gotman J. Intracranial electroencephalographic seizure-onset patterns: effect of underlying pathology. *Brain*. 2014;137(1):183-196. doi:10.1093/brain/awt299

10. Lagarde S, Buzori S, Trebuchon A, et al. The repertoire of seizure onset patterns in human focal epilepsies: Determinants and prognostic values. *Epilepsia*. 2019;60(1):85-95. doi:10.1111/epi.14604

11. Li A, Huynh C, Fitzgerald Z, et al. Neural fragility as an EEG marker of the seizure onset zone. *Nat Neurosci*. 2021;24(10):1465-1474. doi:10.1038/s41593-021-00901-w

12. Diamond JM, Diamond BE, Trotta MS, Dembny K, Inati SK, Zaghloul KA. Travelling waves reveal a dynamic seizure source in human focal epilepsy. *Brain*. 2021;144(6):1751-1763. doi:10.1093/brain/awab089

13. Bartolomei F, Chauvel P, Wendling F. Epileptogenicity of brain structures in human temporal lobe epilepsy: a quantified study from intracerebral EEG. *Brain*. 2008;131(7):1818-1830. doi:10.1093/brain/awn111

14. Grinenko O, Li J, Mosher JC, et al. A fingerprint of the epileptogenic zone in human epilepsies. *Brain*. 2018;141(1):117-131. doi:10.1093/brain/awx306

15. Izumi M, Ikeda A. Focal ictal direct current shifts by a time constant of 2 seconds were clinically useful for resective epilepsy surgery. *Epilepsia*. Published online 2023.

16. Prerau MJ, Brown RE, Bianchi MT, Ellenbogen JM, Purdon PL. Sleep Neurophysiological Dynamics Through the Lens of Multitaper Spectral Analysis. *Physiology*. 2017;32(1):60-92. doi:10.1152/physiol.00062.2015

17. Prerau MJ, Brown RE, Bianchi MT, Ellenbogen JM, Purdon PL. Sleep Neurophysiological Dynamics Through the Lens of Multitaper Spectral Analysis. *Physiology*. 2017;32(1):60-92. doi:10.1152/physiol.00062.2015

18. Dong X, Yu Z, Cao W, Shi Y, Ma Q. A survey on ensemble learning. *Front Comput Sci*. 2020;14(2):241-258. doi:10.1007/s11704-019-8208-z

19. Magnotti JF, Wang Z, Beauchamp MS. RAVE: Comprehensive open-source software for reproducible analysis and visualization of intracranial EEG data. *NeuroImage*. 2020;223:117341. doi:10.1016/j.neuroimage.2020.117341

20. Wang Z, Magnotti JF, Zhang X, Beauchamp MS. YAEL: Your Advanced Electrode Localizer. *Open Source Tools and Methods*. 2023;10(10).

21. Thomson. Spectrum estimation and harmonic analysis. In: *Proc IEEE*. Vol 70. IEEE; 1982:1055-1096. doi:10.1109/PROC.1982.12433

22. Magnotti JF, Wang Z, Beauchamp MS. RAVE: Comprehensive open-source software for reproducible analysis and visualization of intracranial EEG data. *NeuroImage*. 2020;223:117341. doi:10.1016/j.neuroimage.2020.117341

23. Fischl B. FreeSurfer. *NeuroImage*. 2012;62(2):774-781. doi:10.1016/j.neuroimage.2012.01.021

24. Wang Z, Magnotti JF, Zhang X, Beauchamp MS. YAEL: Your Advanced Electrode Localizer. *eNeuro*. 2023;10(10):ENEURO.0328-23.2023. doi:10.1523/ENEURO.0328-23.2023

25. Diamond JM, Withers CP, Chapeton JI, Rahman S, Inati SK, Zaghloul KA. Interictal discharges in the human brain are travelling waves arising from an epileptogenic source. *Brain*. 2023;146(5):1903-1915. doi:10.1093/brain/awad015

26. Khoo A, De Tisi J, Mannan S, O'Keeffe AG, Sander JW, Duncan JS. Reasons for not having epilepsy surgery. *Epilepsia*. 2021;62(12):2909-2919. doi:10.1111/epi.17083

27. Engel J. What can we do for people with drug-resistant epilepsy?: The 2016 Wartenberg Lecture. *Neurology*. 2016;87(23):2483-2489. doi:10.1212/WNL.0000000000003407

28. Steinbrenner M, Kowski AB, Holtkamp M. Referral to evaluation for epilepsy surgery: Reluctance by epileptologists and patients. *Epilepsia*. 2019;60(2):211-219. doi:10.1111/epi.14641

29. Li A, Huynh C, Fitzgerald Z, et al. Neural fragility as an EEG marker of the seizure onset zone. *Nat Neurosci*. 2021;24(10):1465-1474. doi:10.1038/s41593-021-00901-w

Figure/Table Legends:

Figure 1: FREEZ module results on PT01. 3D brain projection showing marked SOZ channels (1A), as well as the projected multitaper result over time (1B) in the beta frequency range [13 – 30 Hz]. Plots are shown generated from the module with the raw signal over time (1C), multitaper

power result over time per electrode (1D), average power over time line plot (1E), and time plot of the 10th through 100th power percentiles (in steps of 10) for EZ and non-EZ channels (1F), with data from -5 to 10s around seizure onset, which is marked by a green dotted line

Figure 2: FREEZ module workflow. Data and user defined inputs shown in blue, intermediary processes in green, module visualization options in pink, and outputs in orange.

Figure 3: Area under the curve (AUC) for mean power over time from 0 to 20s following seizure onset. Seizure free and non-seizure free patients separated by marked EZ and non EZ channels in the delta (3A), theta (3B), alpha (3C), beta (3D), gamma (3E), and high gamma (3F) ranges. Significant ($P < 0.002$ following Bonferroni correction) pairwise comparisons marked with *.

Figure 4: Machine learning results from the stacked random forest ensemble (SRFE). (4A) Results of leave-one-out patient cross-validation. (4B) Positive predictive value (PPV) vs. true positives (TP) for changing threshold values (shown in blue text), with maximum true positives with PPV ≥ 95% marked by horizontal and vertical dotted red lines, annotated with threshold, TP, false positives (FP), and PPV. (4C) Distribution of feature importance for the SRFE showing mean squared error (MSE) when each base model representing a frequency band was sequentially excluded and the SRFE retrained. (4D) Results of EZ predictions applied to non-seizure free patients showing distribution between resected and non-resected tissue, juxtaposed against seizure-free patients.

Figure 5: Patient multitaper heatmap results in the beta (13 – 30 Hz) range. EZ channels (marked blue) are organized at the bottom of the heatmap and delineated with a blue box. Predicted EZ channels by the random forest are highlighted with an asterisk (*). (5A) PT08, who was seizure-free, had all predicted EZ resected. (5B) PT15, also seizure-free, had one predicted EZ removed, and one not removed. (5C) PT10, who was not seizure-free, had predicted EZ not removed. (5D) PT06, also not seizure-free, had the predicted EZ removed.

Figure 6: Results from patient outcome predictions. 6A displays the Area Under the Curve (AUC) for individual frequency bands calculated using random forests, as well as the AUC for the final stacked random forest ensemble (SRFE) along with accuracy, positive predictive value (PPV), and negative predictive value at the threshold cutoff with maximum accuracy. 6B presents the results from the leave-one-out patient cross validation at the maximum accuracy cutoff, which includes true positives, false positives, true negatives, and false negatives from the SRFE model. 6C illustrates the Pearson correlation coefficients between output probabilities. Finally, 6D shows the statistics over time plots for a seizure free and non-seizure free patient in the beta frequency range [13 – 30 Hz].

Supplementary Table 1: Characteristics of the included patients. Details include demographics, neural recording, surgical procedure, and outcome

Supplementary Table 2: Area under the curve (AUC) average power for included patients in a time window from seizure onset to 20s following seizure onset. Data is mean baselined to a time window -30s to -20s before seizure onset. $P < 0.002$ is considered significant following Bonferroni correction for multiple P-Value testing. * indicates significance.

Supplementary Figure 1: Selection panels provided as user interface options in the FREEZ module. Basic parameter selection options include frequency range, window size, step size, and time-half bandwidth product (1A), while advanced options cover the number of DPSS tapers, minimum allowable NFFT size, taper weights, detrend options, and parallel computing options (1B). Analysis options allow for selection of baselining condition and duration (1C), and analysis frequency and time ranges, with default buttons for predefined ranges in delta (0.5-4 Hz), theta (4-8 Hz), alpha (8-13 Hz), beta (13-30 Hz), gamma (30-90 Hz), and high gamma (90+ Hz) (1D). Plotting options include selection of normalization method, color map, decibel units toggle, definition of seizure onset zone and resect electrodes (colored blue and purple respectively, with overlap in green), grouping of SOZ/Resect channels at the bottom of the map, and toggle for electrode labels (1E). Machine learning options include prediction capabilities and visualization on heatmaps (1F).

Supplementary Figure 2: Machine learning results on electrode selection for multiple models tested machine learning models. Positive predictive value (PPV) (y-axis) vs. true positives (x-axis) for three tested machine learning models on time-frequency features across six frequency ranges (delta, theta, alpha, beta, gamma, high gamma). (2A) Simple random forest model, (2B) frequency-specific random forests with stacked predictions, and (2C) stacked random forest ensemble (SRFE). Blue numbers represent applied thresholds to the output model probabilities. Dotted red lines mark the greatest number of true positives achieved with a PPV ≥ 95% considered the optimal threshold, with intersecting horizontal and vertical dotted red lines specifying the optimal threshold, as well as the number of true positives (TP), false positives (FP), and PPV at that optimal threshold.

(A) Frequency Band and SRFE Patient Outcome - AUC

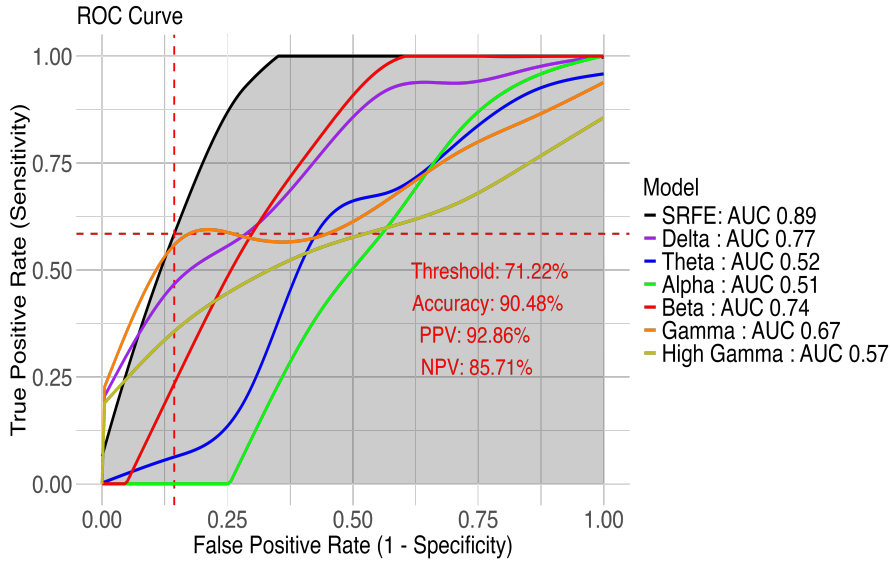

(B) Patient Outcome LOOCV SRFE Results

	Seizure Free	Not Seizure Free
Predicted Seizure Free	13	1
Predicted Not Seizure Free	1	6

(C) Correlation Between Frequency Band Models

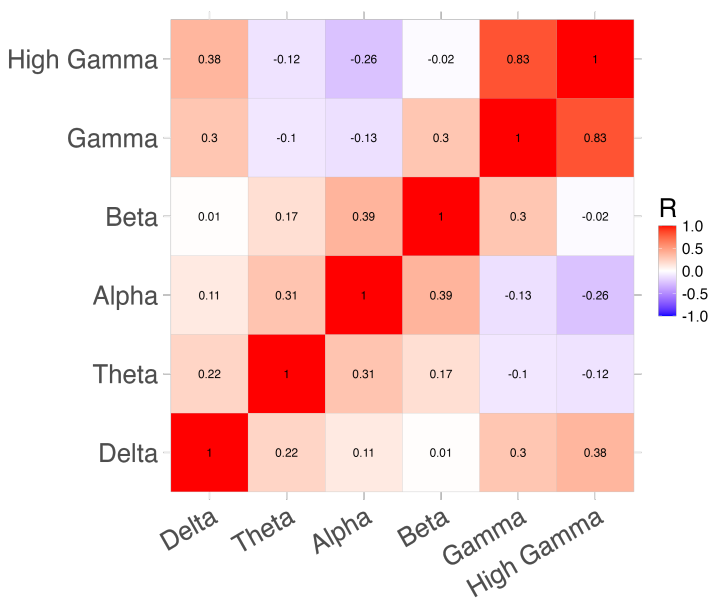

(D) Statistics Over Time Plots

PT8: Seizure Free

Beta [13 - 30Hz]

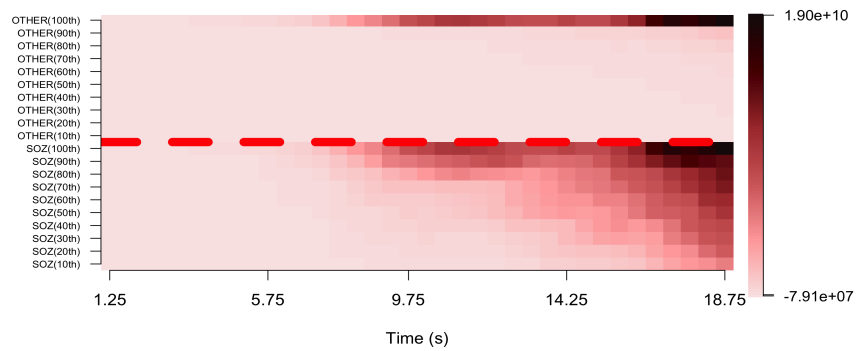

PT10: Not Seizure Free

Beta [13 - 30Hz]

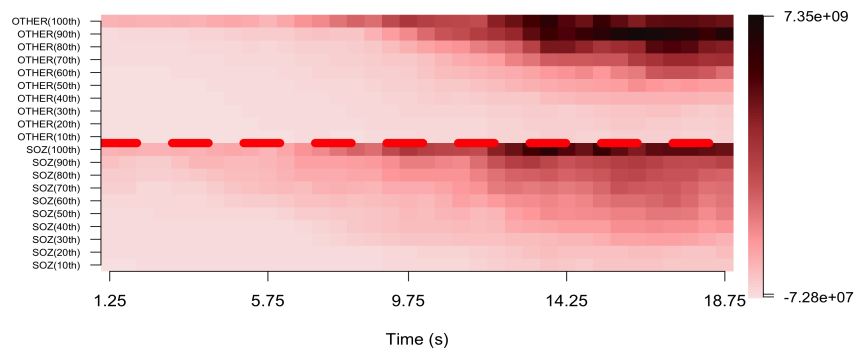

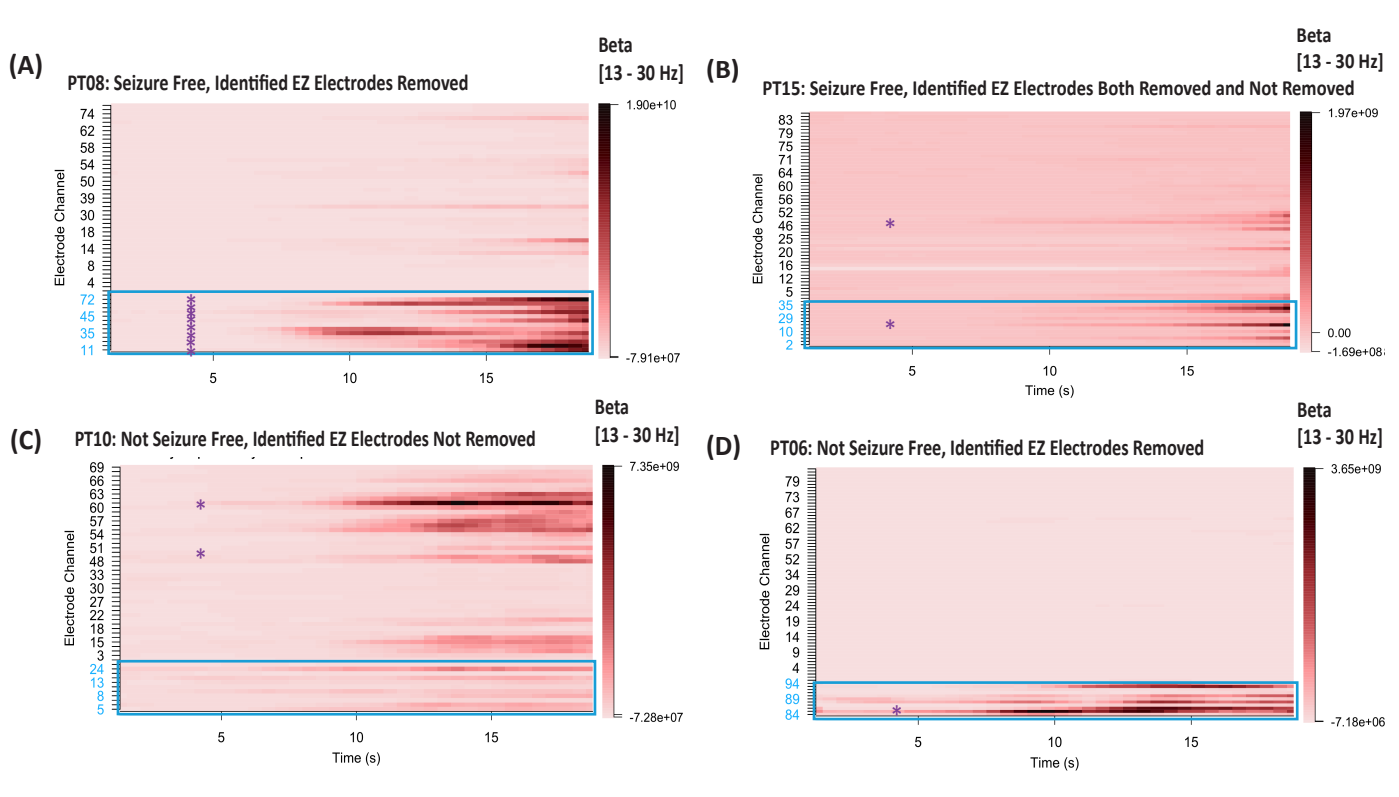
(A)
PT08: Seizure Free, Identified EZ Electrodes Removed
Beta
[13 - 30 Hz]
1.90e+10
-7.91e+07
Electrode Channel
74
62
58
54
50
39
30
18
14
8
4
72
45
35
11
5
10
15
(B)
PT15: Seizure Free, Identified EZ Electrodes Both Removed and Not Removed
Beta
[13 - 30 Hz]
1.97e+09
0.00
-1.69e+08
Electrode Channel
83
79
75
71
64
60
56
52
46
25
20
16
12
5
35
29
10
2
5
10
15
Time (s)
(C)
PT10: Not Seizure Free, Identified EZ Electrodes Not Removed
Beta
[13 - 30 Hz]
7.35e+09
-7.28e+07
Electrode Channel
69
66
63
60
57
54
51
48
33
30
27
22
18
15
3
24
13
8
5
5
10
15
Time (s)
(D)
PT06: Not Seizure Free, Identified EZ Electrodes Removed
Beta
[13 - 30 Hz]
3.65e+09
-7.18e+06
Electrode Channel
79
73
67
62
57
52
34
29
24
19
14
9
4
94
89
84
5
10
15
Time (s)

(A) Seizure Free Patients - LOOCV Results

	EZ	Not EZ
Predicted EZ	22	1
Predicted Not EZ	180	748

(B) Random Forest Stacked Meta-Learner:

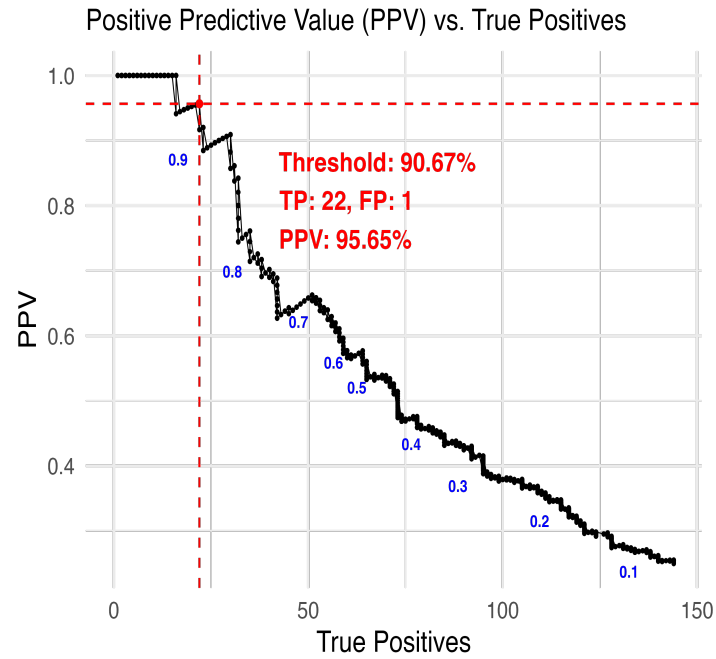

(C) Distribution of Feature Importance Across Folds

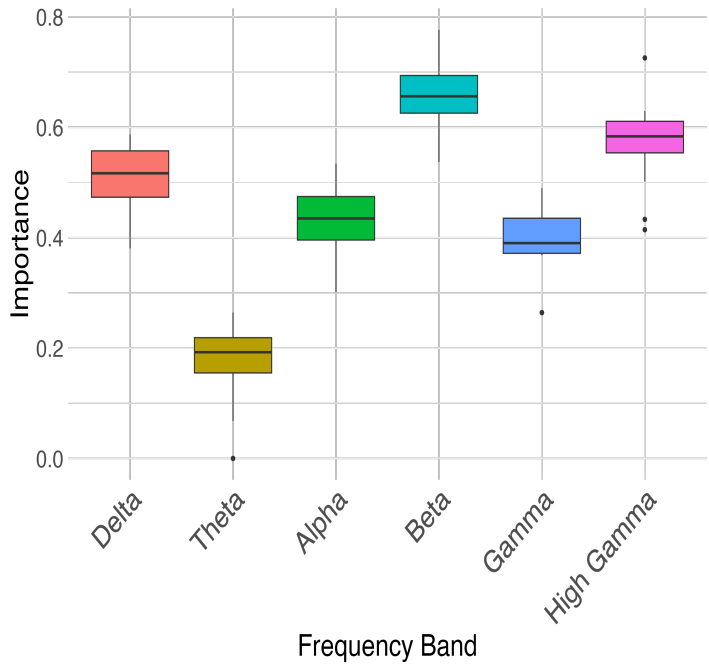

(D) EZ Predictions for Seizure-Free and Not Seizure-Free Patients

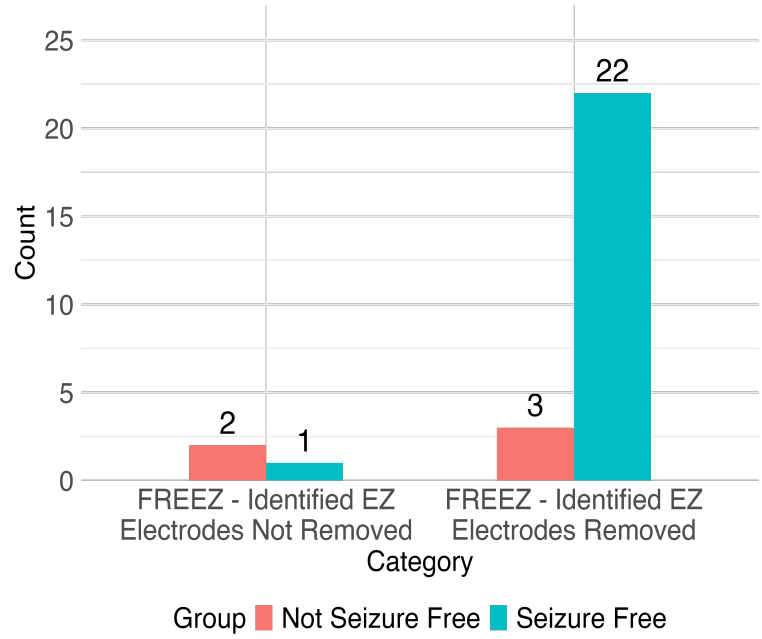

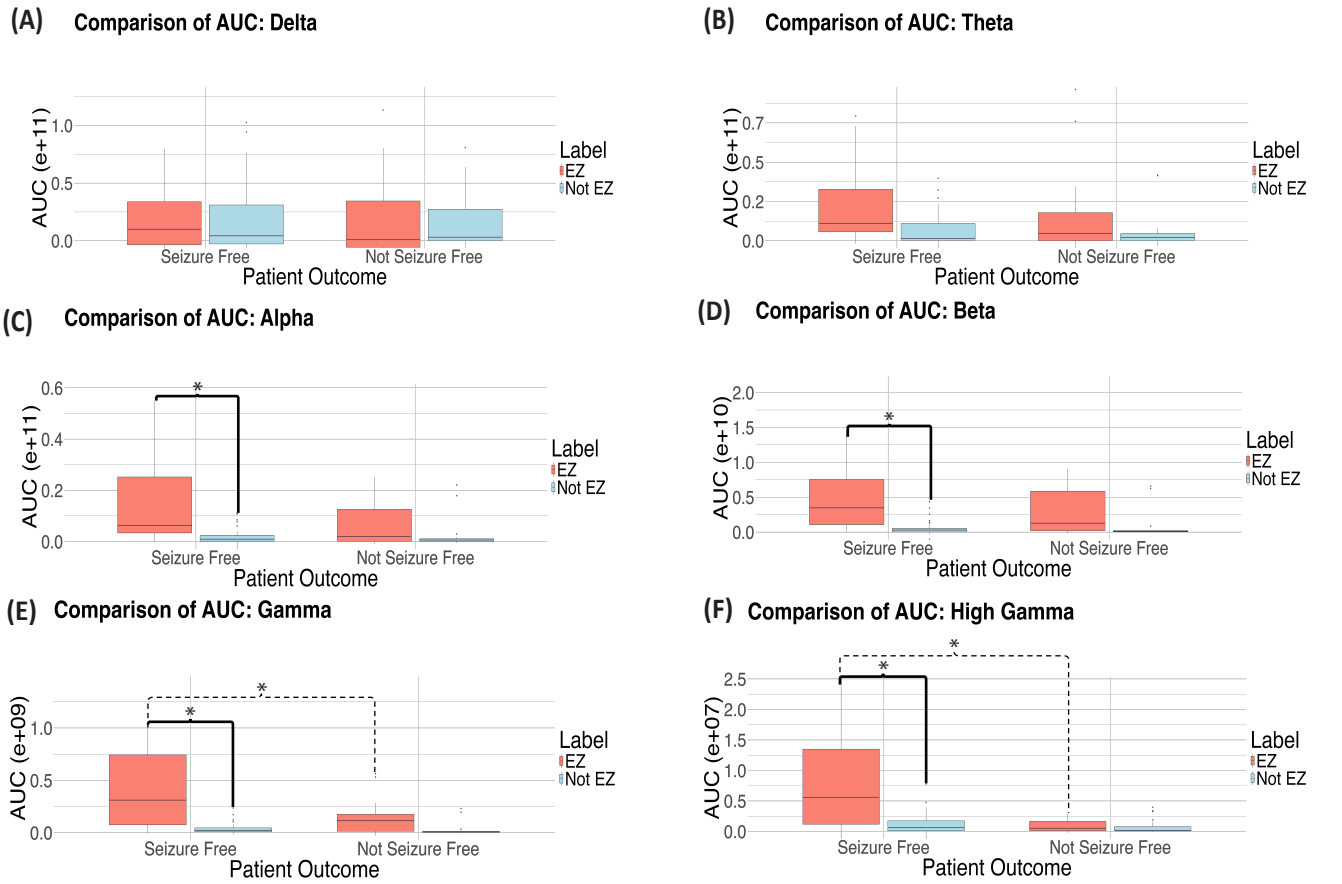
(A) Comparison of AUC: Delta
AUC (e+11)
1.0
0.5
0.0
Seizure Free
Not Seizure Free
Patient Outcome
Label
EZ
Not EZ
(B) Comparison of AUC: Theta
AUC (e+11)
0.7
0.5
0.2
0.0
Seizure Free
Not Seizure Free
Patient Outcome
Label
EZ
Not EZ
(C) Comparison of AUC: Alpha
AUC (e+11)
0.6
0.4
0.2
0.0
*
Seizure Free
Not Seizure Free
Patient Outcome
Label
EZ
Not EZ
(D) Comparison of AUC: Beta
AUC (e+10)
2.0
1.5
1.0
0.5
0.0
*
Seizure Free
Not Seizure Free
Patient Outcome
Label
EZ
Not EZ
(E) Comparison of AUC: Gamma
AUC (e+09)
1.0
0.5
0.0
*
*
Seizure Free
Not Seizure Free
Patient Outcome
Label
EZ
Not EZ
(F) Comparison of AUC: High Gamma
AUC (e+07)
2.5
2.0
1.5
1.0
0.5
0.0
*
*
Seizure Free
Not Seizure Free
Patient Outcome
Label
EZ
Not EZ

FREEZ Module Workflow

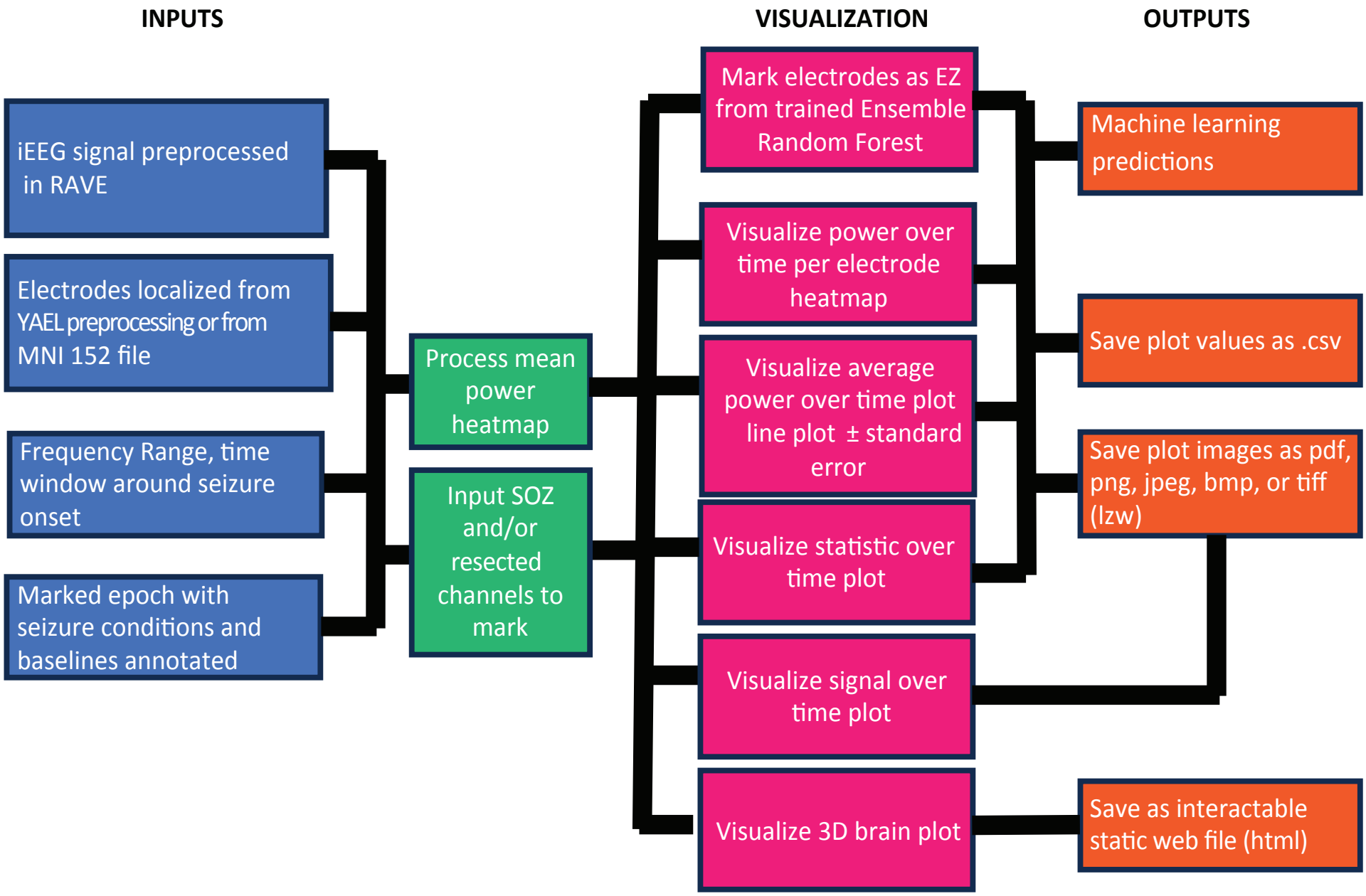

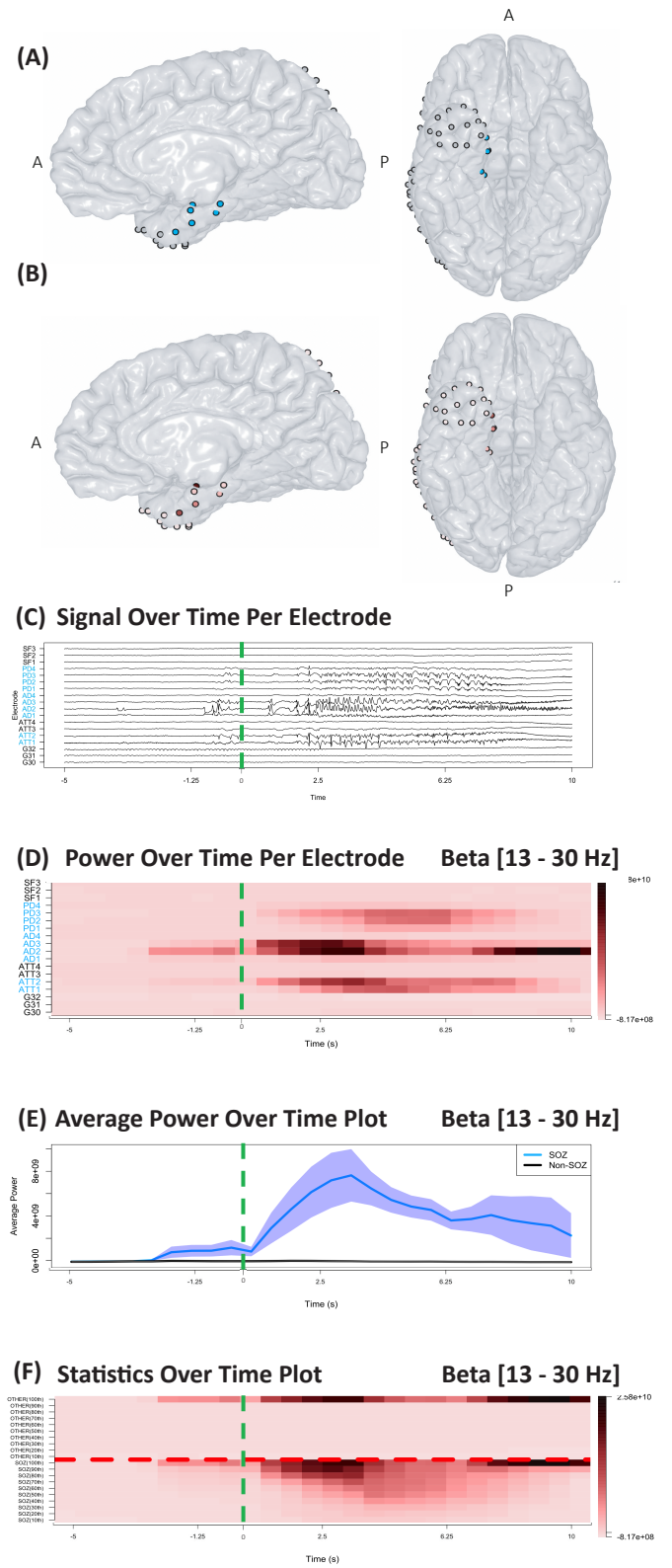
(A)
A
P
A
(B)
A
P
P
(C) Signal Over Time Per Electrode
Electrode
SF3
SF2
SF1
PD4
PD3
PD2
PD1
AD4
AD3
AD2
AD1
ATT4
ATT3
ATT2
ATT1
G32
G31
G30
-5
-1.25
0
2.5
6.25
10
Time
(D) Power Over Time Per Electrode
Beta [13 - 30 Hz]
8e+10
-8.17e+08
Time (s)
(E) Average Power Over Time Plot
Beta [13 - 30 Hz]
SOZ
Non-SOZ
Average Power
8e+09
4e+09
0e+00
Time (s)
(F) Statistics Over Time Plot
Beta [13 - 30 Hz]
2.58e+10
-8.17e+08
Time (s)